Intensity-based pointwise processing in dynamic laser speckle analysis

Intensity-based pointwise processing in dynamic laser speckle analysis

Elena Stoykova*, Natalia Berberova**, Dimana Nazarova** and Atanas Gotchev***

* Korea Electronics Technology Institute, 8Floor, #1599, Sangam-dong, Mapo-gu, Seoul 121-835, Korea

** Institute of Optical Materials and Technologies. Bulgarian Academy of Sciences, Acad. G.Bonchev Str., Bl.109. 1113 Sofia, Bulgaria

*** Tampere University of Technology, Korkeakoulunkatu 10, 33720 Tampere, Finland

e.stoykova@keti.re.kr

Abstract

Intensity-based pointwise algorithms for 2D evaluation of activity in optical metrology with dynamic speckle analysis are studied. They are applied to a temporal sequence of correlated speckle patterns formed at laser illumination of the object surface. A new algorithm is proposed that provides the same quality of the 2D activity map but at less computational effort.

I. INTRODUCTION

Optical metrology with dynamic laser speckle analysis is a promising technique due to variety of applications and simplicity of data acquisition. Coherent illumination of a diffuse object yields a speckle pattern, which changes over time at any object modification. Thus detection of physical or biological activity in various objects (e.g. fruits, seeds, coatings) becomes possible through statistical processing of speckle patterns on their surface [1,2]. If N patterns of size $N_x \times N_y$ are captured for time T at a sampling rate $1/\Delta t = T/N$ and pixel period Δ, then a time sequence of 8-bit encoded intensities $I_{kl,n} \equiv I(k\Delta, l\Delta, n\Delta t), n = 1..N$ is formed at each point $(k\Delta, l\Delta), k = 1..N_x, l = 1..N_y$ of the acquired images. These data can be used to build a pointwise estimate of a given statistical measure by averaging over T. The 2D spatial distribution of the estimate gives a map of object activity.

Inherent feature of any pointwise intensity-based estimate is that it exhibits strong fluctuations from point to point due to speckle nature of the acquired patterns. The fluctuations worsen sensitivity and resolution of the dynamic speckle method as a result of the decreased contrast of the built 2D activity map. Thatôs why the first task of this paper is to study fluctuations and hence quality of the produced activity map in the case of four intensity-based algorithms. The first of them evaluates the so called generalized difference [1] which yields a low-contrast activity map due to the cumulative character of this estimate. The second improves the first one through introduction in calculation of a much shorter than N temporal window and ensures higher contrast [1]. The third algorithm is the recently proposed by us usage of a structure function for a high contrast activity map [2]. We compared these three algorithms in the paper, and, as its second task, we propose a new estimate as a fourth algorithm which provides high quality of the activity map but at less computation time.

II. ACTIVITY MAP QUALITY

The pointwise intensity-based estimates rely on temporal correlation between the laser speckle patterns acquired by the optical sensor. The estimates of the generalized difference and the weighted generalized difference with a window length equal to w are determined from

$$\hat{G}(k,l) = \sum_{i=1}^{N} \sum_{j=i+1}^{N} \left| I_{kl,i} - I_{kl,i} \right|, \quad \hat{G}_w(k,l,w) = \sum_{i=1}^{N-w} \sum_{j=i+1}^{i+w} \left| I_{kl,i} - I_{kl,i} \right| \quad (1)$$

The estimate of the structure function at a time lag m is given by

$$\hat{S}(k,l,m) = \sum_{i=1}^{N-m} \left(I_{kl,i} - I_{kl,i+m} \right)^2 \quad (2)$$

We called our new proposal a modified structure function whose estimate is calculated as

$$\hat{S}_m(k,l,m) = \sum_{i=1}^{N-m} \left| I_{kl,i} - I_{kl,i+m} \right| \quad (3)$$

As it can be seen, the algorithms given by Eq.(2) and Eq.(3) include only one summation and therefore can perform faster than the algorithms given by Eqs.(1). The structure function algorithms could replace calculation of the generalized difference only if they guarantee the same quality of the activity map. Actually they should be compared only to $\hat{G}_w(k,l,w)$ because the window, *w*, as well as the time lag, *m*, introduce selectivity and improves the contrast.

To compare the algorithms, we conducted a numerical experiment with a specially designed synthetic object with varying activity across its surface to have different ratios T/τ_c, where τ_c is the correlation radius of intensity fluctuations. Actually, this ratio measures information capacity provided by a given time sequence. We obtained a correlated sequence of speckle patterns by i) generation of a sequence of 2D spatially delta-correlated random phase distributions $\varphi(k,l,n)$ at a normalized temporal correlation function $R(\tau) = \exp[-\tau/\tau_c]$; phase evolution was introduced as is described in [3]), ii) simulation of subjective speckle intensity at the CCD aperture. The complex amplitude of the light reflected from the object was modeled as $U_S = \sqrt{I_0}\exp\{-j\varphi\}$ for a laser beam with intensity I_0. In paraxial approximation the complex amplitude at the CCD plane was $U_{CCD} = FT^{-1}\{H \cdot FT(U_S)\}$, where H is the CCD coherent transfer function and $FT[..]$ is the Fourier transform. Integration by the CCD pixels was modeled through summation of values in a 2×2 pixels window. The obtained arrays of 256×256 pixels were saved as 8-bit encoded bitmap images. The patterns of 256×256 pixels were divided into four rectangular regions Z_1, Z_2, Z_3 and Z_4 of size 256×64 pixels each with τ_c taking values of $10\,\Delta t$, $20\,\Delta t$, $40\,\Delta t$ and $80\,\Delta t$. We generated and processed image sequences with $T = 64\Delta t, 128\Delta t, 256\Delta t, 512\Delta t$.

To evaluate fluctuations of the estimates we built their histograms at assumption that any activity map has 256 levels. We show in Fig.1 and Fig.2 exemplary histograms obtained for the four algorithms in the case of processing the regions Z_1 and Z_4 from the test object at $T = 256\Delta t$. Figure 3 presents activity maps which correspond to the histograms. The maps show the four regions of different activity in the test object. We see that the histograms for the estimate of the generalized difference overlap to a large degree even at the substantial difference in the correlation radii in Z_1 and Z_4. Therefore the regions of different activity are practically indiscernible in the activity map built by this algorithm (Fig.3). The Figure 1 shows also the histograms for the estimate of the weighted generalized difference that has been calculated with a window of 4 samples. The contrast of the activity map for this algorithm is strongly increased. The spread of the histograms for the estimate $\breve{\mathcal{E}}_w(k,l,w)$ decreases with the correlation radius; for $\breve{\mathcal{E}}(k,l)$ the spread is more or less the same in all activity regions. The structure function as a measure of activity ensures a good contrast activity map (Fig.3). The characteristic feature of this estimate is the strong dependence of the spread of the histograms on the correlation radius.

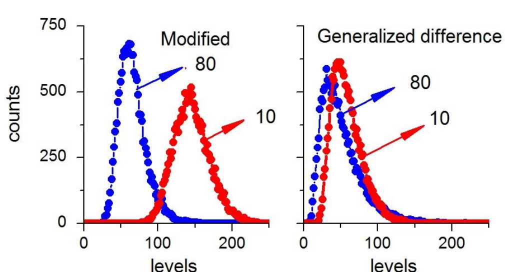

Fig.1. Histograms of the estimates given by Eqs.(1) in the test object regions with correlation radii $10\,\Delta t$ and $80\,\Delta t$. The weighted generalized difference is evaluated at a window length of 4 samples.

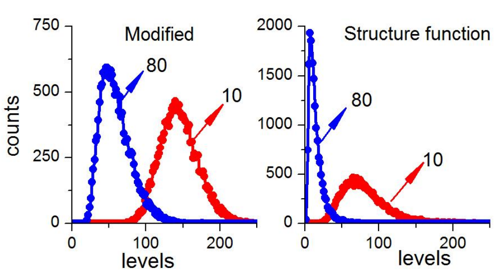

Fig.2. Histograms of the estimates given by Eqs.(2) and (3) in the test object regions with correlation radii $10\,\Delta t$ and $80\,\Delta t$. The structure function and its modified version are evaluated at a time lag $4\,\Delta t$.

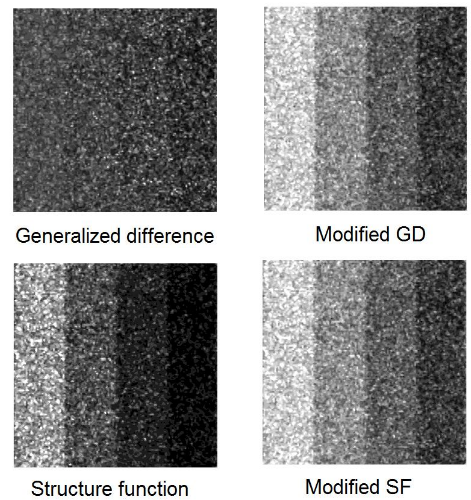

Fig.3. Activity maps for a test object with four regions of activity at processing by intensity-based pointwise algorithms. The spatial distributions of the estimates are normalized to the maximal observed value, and the maps show variation of the parameter from 0 to 1.

Comparison of the histogram of the estimate (3) to that of $\breve{\mathcal{E}}_w(k,l,w)$ proves that both histograms practically coincide. The same is obtained at $T = 64\Delta t, 128\Delta t,, 512\Delta t$. Increase of the window length or of the time lag leads to gradual rise in the histogram spreads for both algorithm, but they continue to provide comparable quality of activity maps. This means that the algorithm (3) can successfully replace calculation of the weighted generalized difference.

We applied the considered intensity-based algorithms to processing of raw data acquired for real objects. The activity maps of the weighted generalized difference, structure function and the modified structure function were characterized with a good contrast. The main drawback of these algorithms is their vulnerability to non-uniform illumination and varying reflectivity across the object.

Acknowledgment

The work is supported by the Academy of Finland, grant No. 137012: High-Resolution Digital Holography: A Modern Signal Processing Approach..

References

[1] F. Saúde, F. de Menezes, P. Freitas, G. Rabelo, and R. Braga, "Alternative measures for biospeckle image analysis," *JOSA A* , vol.29, pp. 1648-1658, August 2012.

[2] E. Stoykova, B. Ivanov, and T. Nikova, "Correlation-based pointwise processing of dynamic speckle patterns," *Opt. Lett.* , vol. 39, pp. 115-118, Jan. 2014.

[3] A.Federico, G.H. Kaufmann, G.E. Galizzi, H. Rabal, M. Trivi, R. Arizaga, ñSimulation of dynamic speckle sequences and its application to the analysis of transient processesò, *Opt.Commun.* vol.260, pp.493-499, April 2006
E. Equis, P. Jacquot, ñSimulation of speckle complex amplitude: advocating the linear modelò, *Proc. SPIE* vol.6341, pp. 634138-1-6, 2006